**Al-Rafidain Journal of Engineering Sciences**

**Journal homepage https://rjes.iq/index.php/rjes**

**ISSN 3005-3153 (Online)**

# Preparation of Eco-Friendly Activated Biochar using Peach Kernal as an Adsorbent for Phenols from Waste Water

Sarah Asif Abdullah [1], Zainab Abdul Razak Naser[2] , Nagam Obaid Kariem [3]

[1]Environmental Engineering Department, College of Engineering, Mustansiryiah University, Baghdad, Iraq.
[2,3]Mustansiryiah University, College of Engineering, Baghdad, Iraq.

**ARTICLE INFO**

***Article history:***
Received 23 June 2023
Revised 23 June 2023,
Accepted 30 June 2023,
Available online 01 July 2023

***Keywords:***
Adsorption
Activated biochar
Chemical activation
Phenol
peach Kernel

**ABSTRACT**

This study investigates the synthesis and application of eco-friendly activated biochar derived from peach kernels (PK) for the removal of phenol from wastewater. The PK material was chemically activated using phosphoric acid and characterized using FTIR, SEM, BET, and XRD techniques. The activation process significantly enhanced the adsorbent's surface area (from 0.54 to 928.47 m²/g) and porosity, as confirmed by BET analysis. Batch adsorption experiments revealed that phenol removal efficiency improved dramatically after activation, reaching over 99% under optimal conditions (pH 3–5, 200 rpm, 0.8 g dose, and 90–150 min contact time). Adsorption isotherm studies indicated that the Langmuir model best fit the experimental data ($R^2 = 0.9973$), suggesting monolayer adsorption. Kinetic analysis showed that the adsorption followed a pseudo-second-order model ($R^2 = 0.999$), indicating that chemisorption was the dominant mechanism. The findings highlight the potential of peach-kernel-derived activated biochar as an efficient and sustainable adsorbent for phenol removal in water treatment applications.

## 1. Introduction

With the rapid growth of industrial society, environmental pollution has become an increasingly critical issue [1], [2]. Among various forms of pollution, water contamination is of particular concern due to its direct impact on human health [3], [4]. Industrial and urban development, while essential for economic progress, have also emerged as major sources of water pollution [5], [6]. Phenol is one such hazardous pollutant, recognized for its toxicity and potential carcinogenicity, even at low concentrations[7]. Major sources of phenol in wastewater include chemical, petrochemical, pharmaceutical, paper, textile industries, and domestic waste[8] .

Various treatment methods exist, yet adsorption has proven to be one of the most effective due to its simplicity, cost-efficiency, and availability of diverse adsorbents [9], [10]. Activated biochar, in particular, has gained attention for its high adsorption capacity, attributed to its heterogeneous surface and abundance of functional groups ([11], [12]. Using biochar derived from fruit waste offers an eco-friendly approach to phenol removal while contributing to

Corresponding author E-mail address: sara_assif4@uomustansiriyah.edu.iq
https://doi.org/10.61268/g0pv8q51

waste reduction and circular economy strategies[13]. The porous structure and active sites of fruit waste–based biochar enhance its potential in wastewater treatment applications [14],supporting global efforts toward sustainable water management [15].

## 2. EXPERMINTAL WORK

### *2.1. Collection and preparation of peach kernel (PK)*

Collected peach kernel then broken to extract the seeds inside after that washed with distilled water to remove the dust and unknown substances then dried in oven at 105 C° for 24 h figure (3-3)(A) then ground in a grinder into a fine powder and sieved to particles < 1mm to prepare the adsorbents before activation process (3-3)B . [16] Figure 1(b).

**a)** **b)**

**Figure 1**. step preparation (PK) before activation process

### *2.2. Chemical activation process*

The use of phosphoric acid ($H_3PO_4$) with concentration of 85% in the activation of activated biochar has sparked widespread interest due to its usefulness in improving the adsorptive capacities of activated biochar for various pollutants, particularly phenolic chemicals. As a dehydrating agent, phosphoric acid promotes the creation of a porous structure within the carbon matrix obtained from agricultural leftovers, hence increasing both surface area and porosity. This property is critical because a bigger surface area usually results in a greater number of active sites available for adsorption.[17].

According to [18], activated biochar was generated utilizing the PK chemical activation procedure with phosphoric acid ($H_3PO_4$). In brief, 100 g of crushed PK was soaked in phosphoric acid at a 1:3 (w/w) ratio. The mixture was slightly stirred to ensure acid penetration, heated to 70◦C for 2 hours, then left overnight at room temperature. The mixture was placed in a muffle furnace and heated to 500◦C for 2 hours at a rate of 5◦C per minute. The acid was removed with distilled water until the pH was 6.8.The activated charcoal was dried at 105◦C for 24 hours using an electric oven. So, the substance is ready after activation. Figure 2**.**

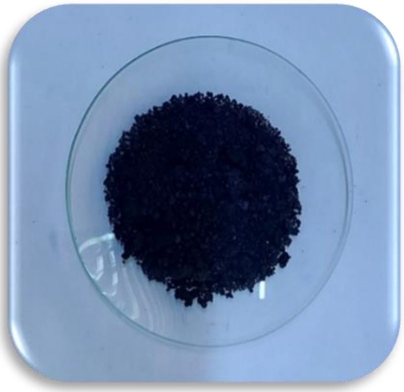

**Figure 2**. preparation (PK) after activation process

### *2.3. Preparation of stock solutions:*

To avoid any additional pollutants or materials that could affect the accuracy and quality of the results, the adsorption experiments were carried out by preparing previously prepared simulated solutions with the required concentrations, as well as a stock solution containing 1000 ppm phenol. Amount of 1 g of phenol A was dissolved in one liter of distilled water [19]. The dissolving procedure was carried out manually for 15 minutes at room temperature

### *2.4. Characterization techniques*

The samples were analyzed before and after activation using a variety of techniques to determine structural and surface changes. The analyses included FTIR for functional group identification, SEM for morphology and surface investigation, BET for surface area and porosity assessment, and XRD for crystalline structure study. These methodologies enabled a thorough assessment of the impact of activation on material characteristics.

## 3. RESULTS AND DISCUSSRION

### *3.1. Adsorbent Characteristics*

### *3.1.1. FTIR test*

The FTIR spectra before activation, after activation, and after phenol adsorption are shown in Figure 3. The wide OH stretch peaks observed at 3416 cm-1 before and after activation are attributed to alcohols present in the lignocellulosic matrix as well as absorbed water. However, following the adsorption of phenol, this absorption band will overlap with the adsorbed phenolic hydroxyl groups. The peak intensities of the OH groups in the activated sample were lower than those in the unactivated sample. C=C bonds may be responsible for the intense peaks around 1635 cm−1. The peak at 1751 $cm^{-1}$ can be associated with the carbonyl group of esters. Before the activation sample, the double peaks around 2926 and 2852 $cm^{-1}$ may correspond to the asymmetric and symmetric stretching of CH2 and CH3 groups, respectively, as well as their bending vibration around 1465 $cm^{-1}$. Compared to the prior activation sample, sharper peaks were seen at 1117 after activation, indicating a rise in functional groups with single oxygen bonds, such ethers, esters, alcohols, phenols, and lactones. The peaks at 1383 $cm^{-1}$ and 1465 $cm^{-1}$ correspond to the methyl rock (1382 $cm^{-1}$) and CH scissoring (1468 $cm^{-1}$), respectively.

The OH peak, which is less prominent after activation and adsorption, suggests that the activation process has improved specific characteristics of the base material.

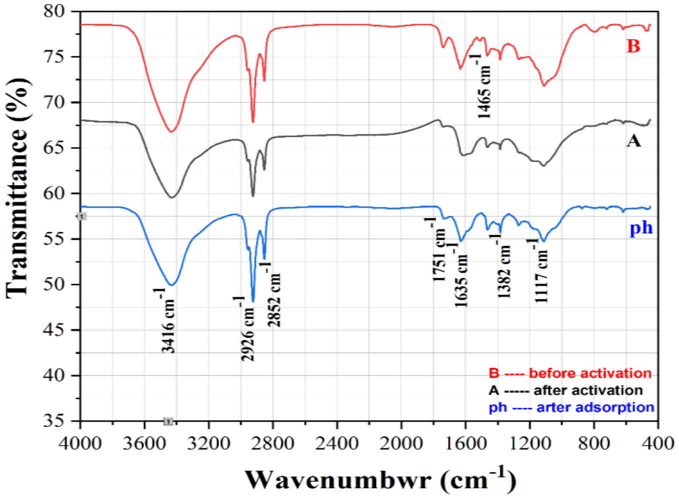

**Figure 3.** The FTIR spectrum of PK

***3.1.2. SEM***(SEM) analysis was conducted to investigate the morphological changes of the material before and after activation. The pre-activation SEM images revealed a rough and non-uniform surface morphology, characterized by the presence of large, irregular agglomerates and visible interparticle voids see in figure (4-5)A. These features indicate that the material had not yet undergone effective dispersion or structural refinement. The particle size, measured at approximately 77.42 nm, was relatively large for nanoscale materials, and the lack of homogeneous distribution suggested limited surface area and reduced reactivity see in figure (4-5)C.

Following activation, the SEM images demonstrated significant structural transformations. The surface appeared markedly rougher, with improved particle dispersion and enhanced porosity see in figure (4-5)B. Notably, the average particle size decreased to approximately 47.88 nm, see in figure (4-5)D indicating that the activation process effectively disintegrated the larger agglomerates into smaller, more uniformly distributed nanoparticles. This structural refinement is expected to enhance the material’s surface area and active sites, thereby improving its performance in applications such as catalysis, adsorption, or energy storage.

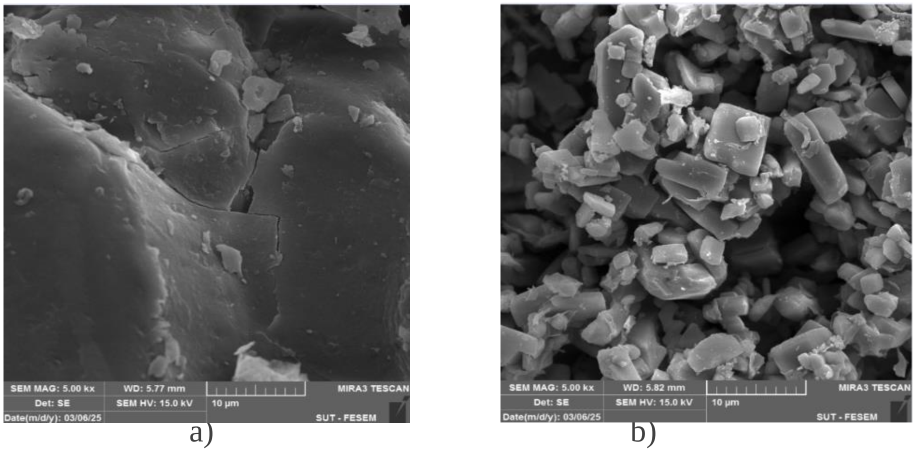

a)

b)

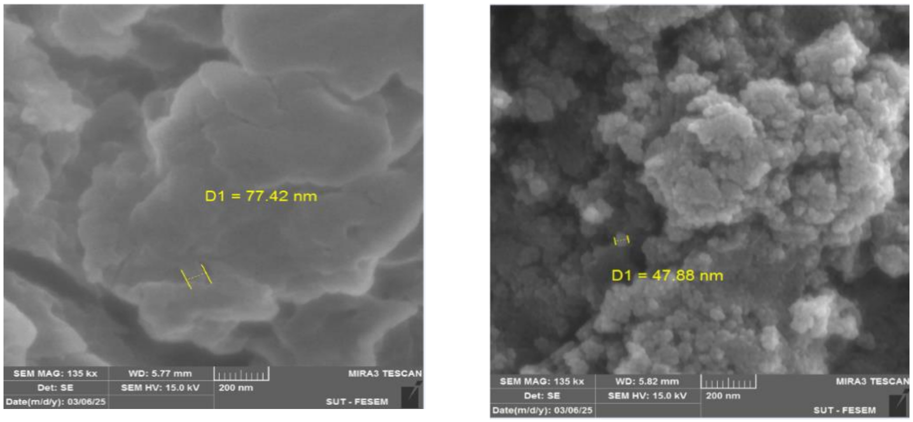

c) d)

**Figure 4.** The SEM of PK ,(a and b) before activation ,(b and c) after activation

### *3.1.3. Brunauer–Emmett–Teller (BET)*

The results showed in table 1 a good increase in surface area, as the surface area increased from 0.54655 m²/g before activation to 928.47 m²/g after activation, which reflects the high efficiency of the activation process in opening the pores and increasing the adsorption efficiency of the material. The results also showed that the pore volume doubled from 0.00277005 cm³/g to 0.6988 cm³/g, which is a significant improvement indicating the formation of a new internal pore network after activation. The results also showed that the average pore diameter decreased (from 19.764 nm to 3.0105 nm), which indicates the structure shift from mesopores/macropores to micropores, which is common after charcoal activation.

The above improvement in properties makes this material suitable and promising for adsorption, pollutant removal and storage applications within the adsorbent.

**Table 1 .** Main results of BET analysis

| | property | Before activation | After activation |
|---|---|---|---|
| 1 | Average pore diameter | 19.764 nm | 3.0105 nm |
| 2 | Langmuir area | 0.5717 m²/g | 863.94 m²/g |
| 3 | Surface area (BET) | 0.54655 m²/g | 928.47 m²/g |
| 4 | Total pore volume | 0.0027005 $cm^3/g$ | 0.6988 $cm^3/g$ |

### *3.1.4. X-ray Diffraction (XRD)*

The XRD pattern before phenol adsorption shows varying peak intensities across different 2θ angles, which reflects the crystalline arrangement of the material. The peaks represent distinct crystal planes and their corresponding spacings, indicating the material's original structure. After phenol adsorption, the XRD pattern(Blue Curve) in figure (4-8) hows noticeable changes in peak intensities at certain 2θ angles. These changes suggest that phenol adsorption has affected the material's crystal structure, potentially altering the spacing between the crystal planes or the overall arrangement. The increase or decrease in peak intensity indicates that adsorption may have caused structural rearrangements or changes in the phase composition. (Red curve) in figure (4-8).

The comparison between the two patterns clearly demonstrates the impact of phenol adsorption on the crystalline properties of the material, highlighting the structural modifications that occurred during the adsorption process.

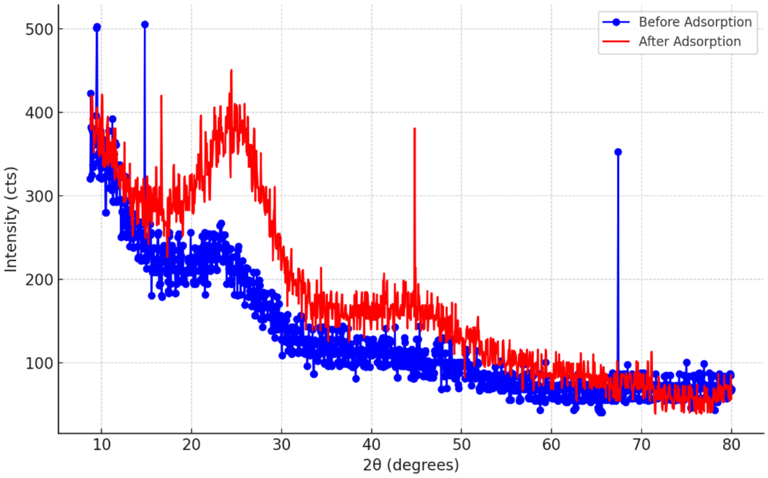

**Figure 5.** The (XRD) Analysis PK , before and after phenol adsorption

## *3.2 Batch adsorption studies for Phenol removal*

### *3.2.1. PH Levels Tested*

The effect of pH on phenol removal efficiency was investigated before and after the activation process. The results demonstrated a significant improvement in adsorption capacity following activation. Before activation, the removal efficiency was notably low across all pH levels, with a maximum of only 8.1% at pH 3 and decreasing to 2.02% at pH 11. However, after activation, the material exhibited a remarkable increase in removal efficiency, reaching over 99% at acidic pH levels (99.252% at pH 3 and 99.718% at pH 5). Although the efficiency slightly decreased with increasing pH, it remained high, maintaining values of 92.252%, 89%, and 86.7% at pH 7, 9, and 11, respectively. This notable enhancement indicates that activation significantly improved the surface properties of the adsorbent (Memon et al., 2008)

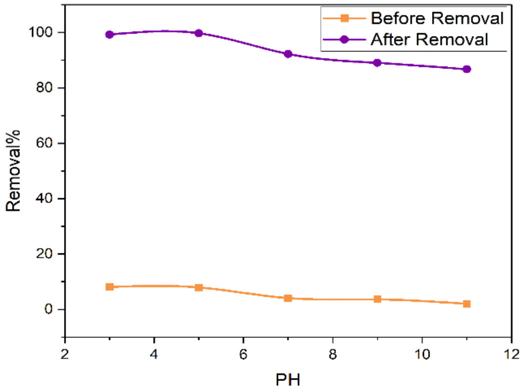

**Figure 6.** Effect of Acidic Function (pH) on Removal of phenol by PK before activation and after activation, At (initial phenol concentration 50 mg/l, adsorbent dosage 0.8 g , contact time 120 min and speed 200 rpm)

### *3.2.2. Contact Time*

The impact of contact time on phenol removal efficiency was evaluated over a range of 30 to 150 minutes, revealing substantial improvements after the activation of the adsorbent. Prior to activation, the removal efficiency remained low throughout the time intervals, peaking at 8.1% at 90 minutes and then declining, suggesting limited adsorption capacity and active site availability. In contrast, after activation, the adsorbent exhibited a significant enhancement in removal efficiency, starting at 85.89% at 30 minutes and reaching a maximum of 99.964% at 150 minutes. The sharp increase between 30 and 60 minutes (from 85.89% to 99.634%) indicates a rapid adsorption phase, followed by a plateau, suggesting saturation of active sites. These findings highlight that activation greatly enhanced the adsorbent's surface characteristics, facilitating faster and more efficient phenol uptake over time. [20]

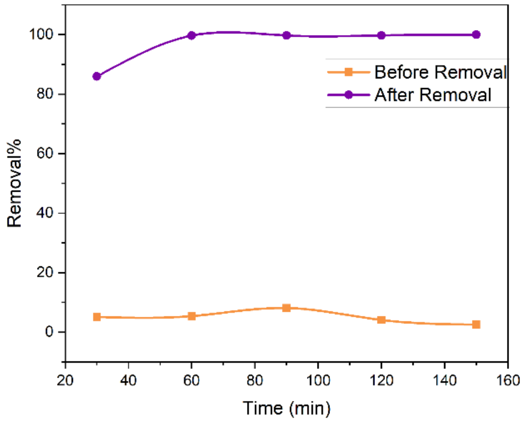

**Figure 7.** Effect of time on Removal of phenol by pk before activation and after activation, At (initial phenol concentration 50 mg/l, adsorbent dosage 0.8 g , PH 7, and speed 200 rpm)

### *3.2.3. Agitation Speed*

The influence of agitation speed on phenol removal efficiency was assessed at different speeds ranging from 100 to 250 rpm. Before activation, the removal efficiencies were consistently low, ranging from 2.3% to 6.132%, with only slight improvements as speed increased. After activation, however, a substantial enhancement in performance was observed. The adsorption efficiency increases significantly (from 2.8% to 99.99%) when the rpm increased from 100 to 250 rpm. This trend indicates that higher agitation speeds improved the dispersion of adsorbent particles, reduced boundary layer resistance, and enhanced mass transfer rates, thereby facilitating more effective phenol adsorption post-activation.[21]

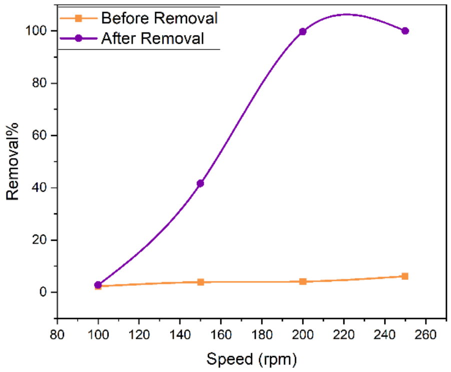

**Figure 8.** Effect of agitation speed on Removal of phenol by pk before activation and after activation, At (initial phenol concentration 50 mg/l, adsorbent dosage 0.8 g , contact time 120 min speed 200 rpm)

### *3.2.4. Initial phenol concentration*

The effect of initial phenol concentration on removal efficiency was studied in the range of 50 to 250 mg/L. Prior to activation, the adsorbent exhibited very low removal efficiencies, ranging from 4.1% at 50 mg/L to as low as 1.29% at 250 mg/L, indicating limited adsorption capacity and active site availability. After activation, a significant improvement was observed, with removal efficiency reaching 99.718% at the lowest concentration (50 mg/L). However, as the initial phenol concentration increased, the removal efficiency gradually declined to 68.16% at 250 mg/L. This inverse relationship can be attributed to the saturation of available adsorption sites at higher concentrations, where the fixed number of active sites becomes insufficient to adsorb the increasing number of phenol molecules. The results confirm that while activation enhances the adsorbent's capacity, its performance still depends on the initial pollutant load, with higher concentrations requiring either higher doses of adsorbent or longer contact times for optimal removal. . [22]

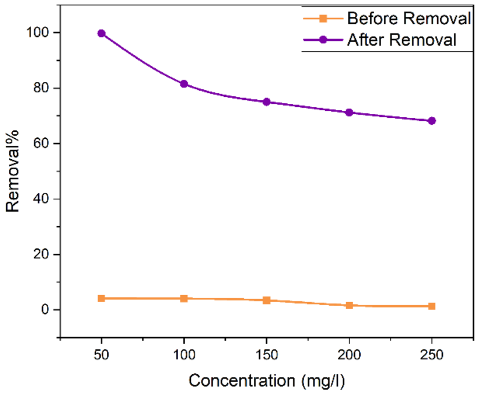

**Figure 9.** Effect of initial concentration on Removal of phenol by pk before activation and after activation, At (PH 7, adsorbent dosage 0.8 g , contact time 120 min speed 200 rpm)

### *3.2.5. Dosage of adsorbent*

The effect of adsorbent dose on phenol removal efficiency was examined using doses ranging from 0.4 to 1.2 g. Prior to activation, removal efficiency was generally low, increasing slightly with higher doses—from 3.16% at 0.4 g to 9.36% at 1.2 g—indicating a limited availability and effectiveness of the native adsorbent surface. After activation, a dramatic improvement in removal performance was observed. The removal efficiency rose from 67.22% at 0.4 g to over 99.7% at doses of 0.8 g and above. This enhancement is attributed to the increased number of active sites and improved surface characteristics following activation. The data also suggest that beyond a certain dosage (0.8 g), the system approaches saturation, as further increases in dose do not significantly improve removal efficiency. This behavior confirms that activation greatly enhances adsorbent effectiveness, and that 0.8 g can be considered an optimal dose under the given conditions. [23]

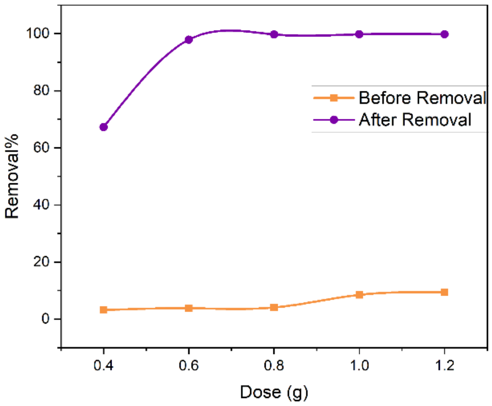

**Figure 10.** Effect of dose on Removal of phenol by pk before activation and after activation, At (initial phenol concentration 50 mg/l, PH 7 , contact time 120 min speed 200 rpm

### *3.3. Adsorption Isotherm Models*

The adsorption equilibrium data were analyzed using four isotherm models: Langmuir, Freundlich, Temkin, and Dubinin–Radushkevich (D–R). Among these, the Langmuir model showed the best fit to the experimental data, with the highest coefficient of determination ($R^2 = 0.9973$), indicating excellent fitting quality. This suggests that the adsorption process predominantly follows a monolayer adsorption mechanism on a homogeneous surface with a finite number of identical sites.

The Freundlich and Temkin models both provided reasonably good fits, with $R^2$ values of 0.9751 and 0.9752, respectively, reflecting good fitting quality. The Freundlich model implies a heterogeneous surface adsorption and suggests the presence of sites with varying affinities, while the Temkin model points to adsorbate–adsorbent interactions and uniform energy distribution along the surface.

In contrast, the Dubinin–Radushkevich (D–R) model displayed the lowest correlation with the experimental data, with an $R^2$ value of only 0.6786, indicating poor fitting quality. This result suggests that pore-filling or chemisorption mechanisms, typically described by the D–R model, are less dominant in the current system.

Overall, the results confirm that Langmuir adsorption is the most suitable model to describe the behavior of the activated adsorbent used, implying that phenol molecules were likely adsorbed onto a uniform surface through a monolayer mechanism.

**Table 2.** A comparison between adsorption isotherm models

| Model | $R^2$ Value | Fitting Quality | Dominant Mechanism |
|---|---|---|---|
| Freundlich | 0.9751 | Good | Multilayer on heterogeneous surface |
| Langmuir | 0.9973 | Excellent | Monolayer on homogeneous surface |
| Temkin | 0.9752 | Good | Adsorbate–adsorbent interaction |
| D–R | 0.6786 | Poor | Pore filling / Chemisorption (not dominant) |

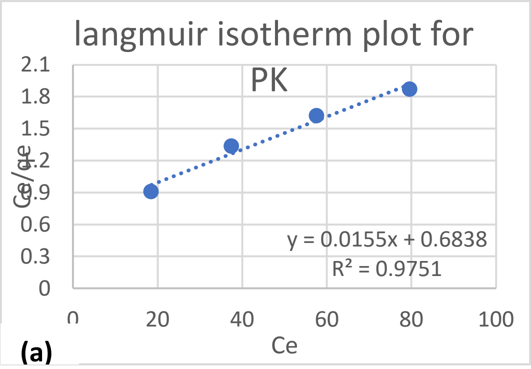

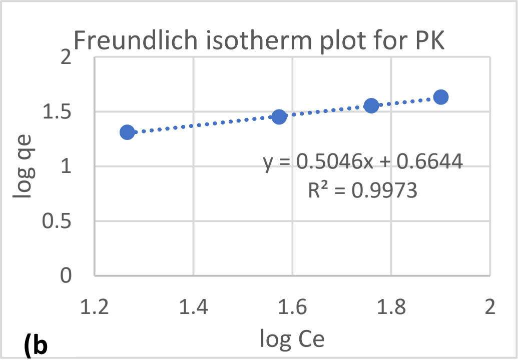

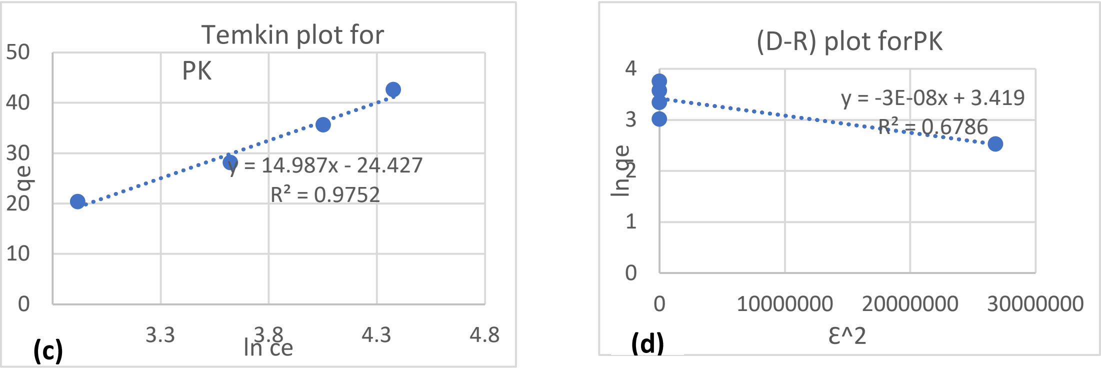

**Figure 11.** Application of Adsorption Isotherm Models ,(a) langmuir isotherm plot ,(b) Freundlich isotherm plot ,(c) Temkin plot ,(d) Brunauer-Emmett-Teller , (e) Dubinin–Radushkevich

## 3.4. *Kinetic Models Analysis*

the adsorption kinetics of phenol onto the activated adsorbent were investigated using three kinetic models: pseudo-first-order, pseudo-second-order, and intraparticle diffusion. The pseudo-second-order model exhibited the best correlation with the experimental data, with an $R^2$ value of 0.999, indicating an excellent fit. This suggests that the adsorption process is likely controlled by chemisorption, involving electron sharing or exchange between phenol molecules and active sites on the adsorbent surface.

In contrast, the pseudo-first-order model showed a very poor fit, with an $R^2$ value of only 0.0125, suggesting it is unsuitable for describing the system. The intraparticle diffusion model yielded a moderate correlation ($R^2$ = 0.864), indicating that while intraparticle diffusion may influence the overall rate, it is not the sole rate-limiting step. Therefore, the adsorption kinetics are best described by the pseudo-second-order model, highlighting the significance of chemical interactions during phenol uptake.

**Table 3. .** A comparison between kinetic models analysis

| Model | $R^2$ Value | Interpretation |
|---|---|---|
| First-order | 0.0125 | Poor fit; model not suitable for this system |
| Second-order | 0.999 | Excellent fit; chemisorption is the dominant mechanism |
| Intraparticle Diffusion | 0.864 | Moderate fit; contributes but not rate-limiting |

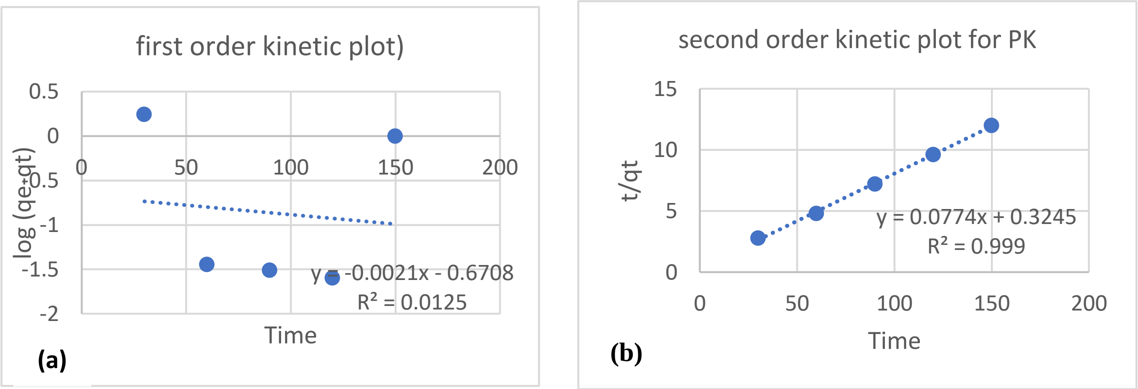

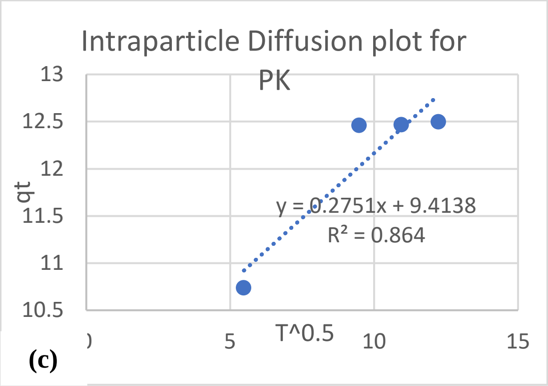

**Figure 12.** Application of Kinetic Models Analysis (a) pseudo-first order kinetic ,(b) pseudo-second order kinetic, (c) Intraparticle Diffusion

## 4. Conclusions

The experimental findings of this study confirm that chemical activation of peach kernel biochar using phosphoric acid significantly improves its physicochemical properties, notably surface area, pore volume, and functional group diversity. These enhancements translated into a substantial increase in phenol adsorption capacity, with removal efficiencies exceeding 99% under optimized conditions. The strong agreement with the Langmuir isotherm model suggests that the adsorption occurred primarily as a monolayer on a uniform surface. Moreover, the pseudo-second-order kinetic model fitting indicates that the rate-limiting step is likely chemisorption involving valence forces through electron exchange or sharing.

The improvement in adsorption performance across various operational parameters—such as pH, contact time, agitation speed, initial concentration, and adsorbent dosage—demonstrates the robustness and adaptability of the activated PK adsorbent. These results highlight the potential of peach kernel waste as a low-cost, sustainable material for water treatment applications**.**

## Acknowledgment

The authors would like to express their sincere appreciation to the Department of Environmental Engineering, College of Engineering, Mustansiriyah University, for providing laboratory facilities and continuous support during this study.

## Reference

[1] G. Saxena, S. P. Goutam, A. Mishra, S. I. Mulla, and R. N. Bharagava, "Emerging and Ecofriendly Technologies for the Removal of Organic and Inorganic Pollutants from Industrial Wastewaters," in *Bioremediation of Industrial Waste for Environmental Safety*, R. N. Bharagava and G. Saxena, Eds., Singapore: Springer Singapore, 2020, pp. 113–126. doi: 10.1007/978-981-13-3426-9_5.

[2] N. O. Kariem, D. E. Sachit, and Z. Q. Ismael, "The performance of a spiral wound RO membrane to desalinate a brackish groundwater in the middle of Iraq," *Desalination Water Treat.*, vol. 136, pp. 72–82, Dec. 2018, doi: 10.5004/dwt.2018.23097.

[3] N. S. Kumar, H. M. Shaikh, M. Asif, and E. H. Al-Ghurabi, "Engineered biochar from wood apple shell waste for high-efficient removal of toxic phenolic compounds in wastewater," *Sci. Rep.*, vol. 11, no. 1, p. 2586, Jan. 2021, doi: 10.1038/s41598-021-82277-2.

[4] M. Nasir, Z. Kadhum, N. Kariem, and Z. Jasim, "Removal of Sesame Oil from Artificial Wastewater Applying Fenton Process and Comparing it with Actual Wastewater," *J. Ecol. Eng.*, vol. 23, no. 10, pp. 248–254, Oct. 2022, doi: 10.12911/22998993/152518.

[5] G. Nirmala, T. Murugesan, K. Rambabu, K. Sathiyanarayanan, and P. L. Show, "Adsorptive removal of phenol using banyan root activated carbon," *Chem. Eng. Commun.*, vol. 208, no. 6, pp. 831–842, Jun. 2021, doi: 10.1080/00986445.2019.1674839.

[6] Hadi Falah Hassan, Khaleel I. Hamad, and Aysar T. Jarullah, "Oxidation of phenol by CWPO method

using nickel manganese oxidecatalyst prepared in glycerol solvent using microwave in batch reactor," *Al Rafidain J. Eng. Sci.*, vol. 3, no. 1, pp. 396–409, Feb. 2025, doi: 10.61268/1sdyb939.

[7] N. Panigrahy, A. Priyadarshini, M. M. Sahoo, A. K. Verma, A. Daverey, and N. K. Sahoo, "A comprehensive review on eco-toxicity and biodegradation of phenolics: Recent progress and future outlook," *Environ. Technol. Innov.*, vol. 27, p. 102423, Aug. 2022, doi: 10.1016/j.eti.2022.102423.

[8] Candan Eryılmaz and Ayten Genç, "Review of treatment technologies for the removal of phenol from wastewaters," *J. Water Chem. Technol.*, vol. 43, no. 2, pp. 145–154, Mar. 2021, doi: 10.3103/S1063455X21020065.

[9] I. I. Salame and T. J. Bandosz, "Role of surface chemistry in adsorption of phenol on activated carbons," *J. Colloid Interface Sci.*, vol. 264, no. 2, pp. 307–312, Aug. 2003, doi: 10.1016/S0021-9797(03)00420-X.

[10] Abdul-Azeez Hatem Mohammed and Haneen A. Kh. Karaghool, "Sustainable Adsorption of Congo Red Dye Using Organic Waste Materials as Green Adsorbents: A Mini-Review," *Al Rafidain J. Eng. Sci.*, vol. 2, no. 2, pp. 78–86, Aug. 2024, doi: 10.61268/tr03jq61.

[11] W. W. Anku, M. A. Mamo, and P. P. Govender, "Phenolic compounds in water: sources, reactivity, toxicity and treatment methods," in *Phenolic Compounds - Natural Sources, Importance and Applications*, M. Soto-Hernández, M. Palma-Tenango, and M. D. R. Garcia-Mateos, Eds., InTech, 2017. Accessed: May 17, 2025. [Online]. Available: http://www.intechopen.com/books/phenolic-compounds-natural-sources-importance-and-applications/phenolic-compounds-in-water-sources-reactivity-toxicity-and-treatment-methods

[12] B. Xie, J. Qin, S. Wang, X. Li, H. Sun, and W. Chen, "Adsorption of Phenol on Commercial Activated Carbons: Modelling and Interpretation," *Int. J. Environ. Res. Public. Health*, vol. 17, no. 3, p. 789, Jan. 2020, doi: 10.3390/ijerph17030789.

[13] N. S. Joodi and N. O. Kariem, "Study of treating the vegetable oils in artificial water using advanced oxidation process," *IOP Conf. Ser. Earth Environ. Sci.*, vol. 1120, no. 1, p. 012031, Dec. 2022, doi: 10.1088/1755-1315/1120/1/012031.

[14] S. Pap *et al.*, "Synthesis of highly-efficient functionalized biochars from fruit industry waste biomass for the removal of chromium and lead," *J. Mol. Liq.*, vol. 268, pp. 315–325, Oct. 2018, doi: 10.1016/j.molliq.2018.07.072.

[15] Z. R. Khanjer, A. H. Ali, and N. O. Kariem, "INVESTIGATING THE ABILITY OF MICROBIAL SOLAR CELL IN ELECTRICAL ENERGY PRODUCTION," *J. Eng. Sustain. Dev.*, vol. 25, no. 1, pp. 123–130, Feb. 2022, doi: 10.31272/jeasd.25.1.11.

[16] K. A. Mohamad Said, A. F. Ismail, Z. Abdul Karim, M. S. Abdullah, and A. Hafeez, "A review of technologies for the phenolic compounds recovery and phenol removal from wastewater," *Process Saf. Environ. Prot.*, vol. 151, pp. 257–289, Jul. 2021, doi: 10.1016/j.psep.2021.05.015.

[17] R. Yang *et al.*, "Experimental investigation of water vapor adsorption isotherm on gas-producing Longmaxi shale: Mathematical modeling and implication for water distribution in shale reservoirs," *Chem. Eng. J.*, vol. 406, p. 125982, Feb. 2021, doi: 10.1016/j.cej.2020.125982.

[18] O. A. Hussain, A. S. Hathout, Y. E. Abdel-Mobdy, M. M. Rashed, E. A. Abdel Rahim, and A. S. M. Fouzy, "Preparation and characterization of activated carbon from agricultural wastes and their ability to remove chlorpyrifos from water," *Toxicol. Rep.*, vol. 10, pp. 146–154, 2023, doi: 10.1016/j.toxrep.2023.01.011.

[19] S. J. Alhamd, M. N. Abbas, H. J. Jawad Al-Fatlawy, T. A. Ibrahim, and Z. N. Abbas, "Removal of phenol from oilfield produced water using non-conventional adsorbent medium by an eco-friendly approach," *Karbala Int. J. Mod. Sci.*, vol. 10, no. 2, May 2024, doi: 10.33640/2405-609X.3350.

[20] G. Z. Memon, M. I. Bhanger, and M. Akhtar, "Peach-nut Shells-An Effective and Low Cost Adsorbent for the Removal of Endosulfan from Aqueous Solutions," vol. 9, no. 2, 2008.

[21] L. Hawal, A. Al-Sulttani, and N. Kariem, "Adsorption of Lead Ions from Aqueous Solutions onto Rice Husks, Continuous System," *J. Ecol. Eng.*, vol. 22, no. 10, pp. 269–274, Nov. 2021, doi: 10.12911/22998993/141936.

[22] M. Afsharnia, M. Saeidi, A. Zarei, M. R. Narooie, and H. Biglari, "Phenol Removal from Aqueous Environment by Adsorption onto Pomegranate Peel Carbon," *Electron. Physician*, vol. 8, no. 11, pp. 3248–3256, Nov. 2016, doi: 10.19082/3248.

[23] A. Ghanadzadeh Gilani, H. Ghanadzadeh, P. Azmoon, and N. Chaibakhsh, "Phenol Adsorption from Aqueous Phase onto Prepared Low-cost Carbons from Natural Sources: A Comparative Study," *Phys. Chem. Res.*, vol. 7, no. 2, Jun. 2019, doi: 10.22036/pcr.2019.160071.1572.